Hydrogen-atom abstractions: a semi-empirical approach to reaction energetics, bond lengths and bond-orders

Alberto A. C. C. Pais, Luis G. Arnaut and Sebastião J. Formosinho *†

Universidade de Coimbra, Departamento de Química, P-3049 Coimbra Codex, Portugal

We propose the use of the Intersecting-State Model (ISM) to estimate activation barriers and reactive bond distances for reactions involving the transfer of hydrogen atoms. The method is used in a variety of systems with transition states of the (H)C–H–C(H), N–H–C(H), O–H–C(H), S–H–C(H), Si–H–C, Si–H–Si, Sn–H–C and Ge–H–C types. Hydrogen abstractions by halogen atoms are also investigated. Results are compared with available experimental, semi-empirical or *ab initio* data. Other transition state types (such as O–H–O) which cannot be properly rationalized in the light of an elementary bond-breaking/bond-forming process are also analyzed.

Introduction

Hydrogen atom transfer reactions are of fundamental importance in several fields of chemistry, for example in many thermal and catalytic processes involving the production of fuels and also in free-radical polymerization. Most of the relevant systems are more easily manageable than other exchange reactions, making them the object of numerous experimental[1] (for a recent example see ref. 2) and theoretical[3–11] studies. The relevance of these reactions has also prompted the study of important properties such as bond strengths and vibrational frequencies in intervening compounds.[12–14]

Up-to-date molecular orbital programs for the calculation of both molecular structure and reaction profiles are readily available. However, these quantitative approaches do not satisfy the chemist's need to understand, unless complemented by simple models shaped to rationalize and predict experimental and computational data. Also, empirical and semi-empirical approaches promote a better discrimination of the various factors that influence the rates of radical reactions and may sometimes be used to estimate reaction rates with accuracies similar to those obtained with more sophisticated methods. The assessment of the factors influencing the reaction energetics in H-atom transfers has gained renewed interest following the debate between Zavitsas and Roberts in a series of articles, most of them appearing in issues of this Journal.[6,15–17]

An early attempt to rationalize energy barriers for this type of reaction was carried out by Evans and Polanyi.[18] These authors recognized that for a homogeneous series of reactions, the energy of the activated state relative to the reagents (E_a) depends linearly on the reaction enthalpy (ΔH^0) where E_0 and α

$$E_a = E_0 + \alpha \Delta H^0 \qquad (1)$$

are constants ($0 < \alpha < 1$). A similar expression was obtained independently by Bell[19] in the context of proton transfer reactions.

This empirical approach to predict activation energies was pursued by other authors.[20] A recent example is the work of Roberts and Steel,[6] which used a fitting procedure of a four-term function to 65 activation energies corresponding to hydrogen abstractions by radicals, 41 of which were carbon radicals. Although this approach leads to small standard

deviations from selected experimental values (≈ 2.0 kJ mol^{-1}), the physical significance of the fitted parameters is open to criticism. The use of those functions to calculate further activation energies sometimes meets with unpredictable failures.[15] These may, however, be sometimes attributed[16] to questionable (experimental or otherwise) reference values rather than to the actual method.

The activation energies of H-atom abstraction reactions have

$$\text{A–H} + \text{B} \longrightarrow \text{A} + \text{B–H} \qquad (2)$$
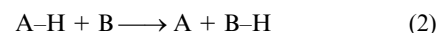
also been estimated using semi-empirical approaches. The most inspiring model in this field is the bond-energy–bond-order (BEBO) method developed by Johnston and Parr.[3,21] This method is based on three empirical relations: (i) the total bond order is conserved during a concerted bond-breaking/bond-forming process; (ii) the bond order (n) of an A–B bond length

$$n_{AH} + n_{HB} = 1 \qquad (3)$$

is related to its bond (l_n) according to the Pauling relationship[22] where l_s is the length of the corresponding single bond and a is

$$n = \exp[-(l_n - l_s)/a] \qquad (4)$$

a "universal" constant; (iii) the bond energy of the AB bond of order n (D_n) is related to the bond energy of the single AB bond (D_s) and to the bond order n where p is an empirical parameter

$$D_n = D_s n^p \qquad (5)$$

that can be estimated from the equilibrium internuclear distance of a rare gas pair and the depth of its Lennard-Jones potential.

The progress variable n can be used in conjunction with eqns. (3)–(5) to calculate the potential energy of an H-atom abstraction at any point of the reaction coordinate. However, in this approximation, some systems present spurious negative activation energies. Johnston and Parr[3] addressed this problem by introducing an anti-Morse function to describe the triplet repulsion between the end atoms of the three-atom fragment involved in the reactive bonds.

A recent evaluation of the BEBO method,[23] involving 97 gas-phase reactions for which experimental activation energies are available, presented an average error of 6.4 kJ mol^{-1} with a standard deviation of 8.2 kJ mol^{-1}.

Another semiempirical approach was proposed by Zavitsas and co-workers.[7,24] The total energy of the system was considered to have four additive contributions: the average bonding energies of AH and HB, the triplet repulsion between A and B and the resonance energy corresponding to the delocalization of an electron, (eqn. 6). The criterion to calculate the energy

$$E_{tot} = 0.5[^1E(AH) + {}^1E(HB)] + {}^3E(AB) + E_r \quad (6)$$

of the system for a given distance l_{AH} is that the corresponding value of l_{HB} satisfies condition (7), being the activation energy

$$^1E(AH) = {}^1E(HB) \quad (7)$$

obtained through minimization of the total energy. This equibonding criterion is only valid for a cut in the potential energy surface of the system that is perpendicular to the reaction coordinate and contains the saddle point. The bonding singlet interactions are described by Morse functions [eqn. (8)],

$$^1E = D_e[\exp(-2\beta r) - 2\exp(-\beta r)] \quad (8)$$

where $r = (l^{\ddagger} - l_{eq})$, and D_e and β are the dissociation energy and Morse decaying parameter, respectively, while the triplet repulsion functions are represented by parametrized anti-Morse potentials. The resonance energy takes two possible values, $E_r = -44.4$ or -50.2 kJ mol^{-1}, depending on whether A or B have atomic number $Z \leq 9$ or $Z > 9$, respectively.

This method of calculating activation energies for H-atom transfer reactions has given results with deviations from the experimental determinations smaller than those corresponding to the original form of the BEBO method. However, it does not provide a reaction coordinate and may in principle be applied only to linear transition states. Also, it is difficult to access the role of the triplet repulsion in situations of hypervalency.[16]

Various *ab initio* and associated semi-empirical methods (see refs. 9 and 10 as recent examples) have also been used to study hydrogen abstractions. Some of these results will be used in the following sections to compare with the present determinations. We note, however, that MNDO-type approaches are not adequate to estimate energy barriers, with typical errors of more than 40 kJ mol^{-1},[25] in comparison to *ab initio* MP3 or MP4 results. Thus, additional scaling is usually necessary[9] and often drastic. In contrast, the same type of method is generally reliable for the estimation of the transition state geometry.

State-of-the-art *ab initio* calculations for relatively small systems[26] present fluctuations in the calculation of energy barriers of several kJ mol^{-1}, as the level of the calculation is increased from medium to highly accurate. Bond lengths at the transition state may also differ by up to 0.20 Å, along the same route. For larger systems, empirical corrections of the SAC-type[27] become indispensable (see, *e.g.* ref. 11) to scale *ab initio* energy results. In general, the corresponding geometries are not corrected. Accurate alternatives like Gaussian-2 theory (see ref. 28 and references therein) also resort to empirical corrections based on experimental atomization energies. The use of semi-empirical and *ab initio* approaches is further discussed in recent articles dealing with free-radical reactivity,[29–32] which also analyze geometries of transition states.

We additionally note that sometimes the relation between 0 K potential energy barriers, calculated at reaction saddle points, and activation energies is not direct, even when zero point energy corrections are considered. For instance, a positive barrier is not incompatible with a negative activation energy.[33,34] Also, when the entrance channel is narrow, a potential energy surface characterized by a purely attractive minimum energy reaction path may give rise to activation energies switching from negative to positive as temperature increases.[35] In most cases, however, the presence of energy barriers clearly determines a positive activation behaviour[36] while the reactivity
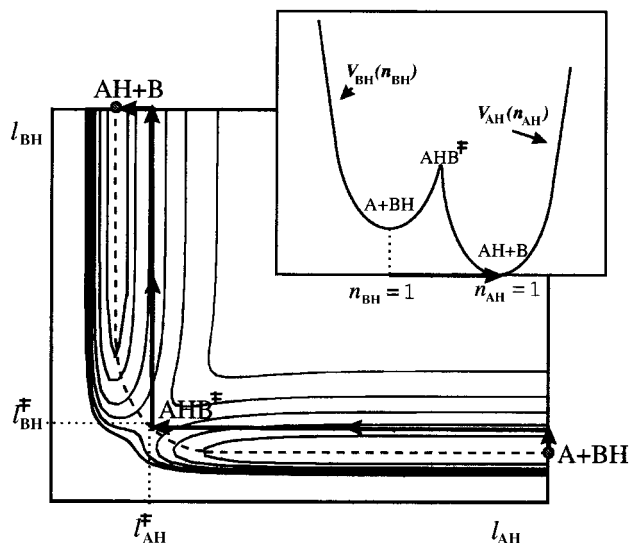

Fig. 1 Schematic representation of the diabatic path connecting reactants and products (the arrows indicate the "Evans–Polanyi diabatic path" and the dashed line the minimum energy path). The insert illustrates the intersection criterion to locate the transition state.

on attractive surfaces is better explained on the basis of, for example, capture-like mechanisms.[37]

In this work we describe and apply a non-parametric version of the Intersecting-State Model (ISM). The present version differs from the original one, published more than ten years ago,[38] in one essential aspect: it does not require parameters from the field of chemical kinetics to calculate the energies of activation of H-abstraction reactions, with an eventual exception (see next section). For practical purposes, the kinetic information can be easily and usefully incorporated.

It should also be noted that only 20 reactions of the type represented by eqn. (2) were originally studied; now this number has been extended to almost 100, including H-abstraction from N, O, S, Si, Sn and Ge. Some of the reactions treated in the early article will be revisited in this work. Applications of the model to other exchange reactions can be found in refs. 39–53.

Our purpose is to go beyond the prediction of energy barriers, and use the model as a probe for different reaction mechanisms. Complementary to the most recent empirical or semi-empirical approaches in which emphasis is given either to various energetic, structural and electronic parameters[6] or to the relevance of a single determining factor,[7] our treatment underlines the importance of the concerted nature of the hydrogen abstraction process and its relation to the equilibrium structure of reactants and products.

Assumptions and theory

The basic assumption behind the use of ISM in these transfer reactions is that the process can be described *via* a bond breaking/bond forming process. This model describes the energy changes along the "diabatic path" of Evans and Polanyi,[18] according to which the AH bond is first stretched to the transition-state configuration and then the HB bond is compressed to its equilibrium value (see Fig. 1).

Following the BEBO model, the transition state is located on the basis of the conservation of the total bond-order ($m = n_{A-H} + n_{B-H} = 1$). Thus, there is a strong correlation between the changes in one bond and the other during the reaction. One of the novelties of ISM is to recognize that long bonds will stretch more than short bonds and that the absolute distension of the bonds to reach the transition state configuration must be scaled by their equilibrium bond lengths. Thus, in order to generalize the Pauling relationship [eqn. (4)] it is necessary to

Table 1 Morse curve parameters used in the present work

System	D_e/kJ mol^{-1}	β/Å^{-1}	l_{eq}/Å	System	D_e/kJ mol^{-1}	β/Å^{-1}	l_{eq}/Å
H$_2$	453.3	1.939	0.741	CH$_4$	453.1	1.947	1.087
C$_2$H$_6$	434.7	1.962	1.094	CH$_3$CH$_2$CH$_3$	425.9	1.968	1.107
(CH$_3$)$_3$CH	413.8	1.972	1.122	C$_2$H$_4$	475.7	1.914	1.071
PhH	478.2	1.918	1.080	PhCH$_3$	382.0	2.091	1.111
NH$_3$	466.1	2.181	1.012	CH$_3$OH	455.2	2.415	0.945
(CH$_3$)$_3$COH	457.7	2.376	0.950	CH$_3$COOH	387.0	2.573	0.960
HOH	516.3	2.200	0.960	HOOH	387.0	2.573	0.960
CH$_3$CHO	387.4	1.993	1.128	CH$_3$COCH$_2$H	418.0	2.028	1.103
H$_2$S	392.9	1.825	1.336	CH$_3$SH	377.4	1.864	1.340
CH$_3$CH$_2$SH	379.1	1.851	1.350	(CH$_3$)$_2$CHSH	378.2	1.817	1.350
PhSH	346.4	1.941	1.360	OH	445.2	2.402	0.971
H$_3$SiH	392.5	1.521	1.480	(CH$_3$)$_3$SiH	404.2	1.439	1.485
[(CH$_3$)$_3$Si]$_3$SiH	358.6	1.833	1.500	(CH$_3$)$_3$SnH	329.3	1.376	1.700
(CH$_3$)$_3$GeH	359.8	1.488	1.535	HF	589.1	2.222	0.917
HCl	445.2	1.872	1.275	HBr	378.2	1.819	1.415
HI	308.4	1.751	1.604				

scale the "universal" constant by the equilibrium bond lengths of the reactive bonds ($l_{A-H,eq}$ and $l_{B-H,eq}$). Thus, in eqn. (4), the parameter a is replaced, in the transition state, by $a'(l_{A-H,eq} + l_{B-H,eq})$, where a' is a dimensionless proportionality constant that has been calibrated,[38] giving $a' = 0.156$. We note that the determination of the value for this parameter could have been made using the H + H$_2$ reaction alone. In any case, this is a concession to the use of kinetic data, required as a starting point for the application of ISM.

We can now relate bond-orders to distorted bonds using the modified Pauling expressions [38] (9) and (10), where $l^{\ddagger}_{(A,B)-H}$ are the A–H and B–H distances at the transition state.

$$n_{A-H} = \exp\left(-\frac{m(l^{\ddagger}_{A-H} - l_{A-H,eq})}{a'(l_{A-H,eq} + l_{B-H,eq})}\right) \quad (9)$$

$$n_{B-H} = \exp\left(-\frac{m(l^{\ddagger}_{B-H} - l_{B-H,eq})}{a'(l_{A-H,eq} + l_{B-H,eq})}\right) \quad (10)$$

Additional stabilization of the transition state ($m > 1$) is included in eqns. (9) and (10) through the use of m in the exponents. The net effect is a reduction in the transition-state bond distensions, which lowers the respective energy. Note that, in this case, n_{A-H} and n_{B-H} become simple progress variables, still adding up to 1 and not to the total bond-order.

The location of the intersection between reactant and product curves is obtained when eqn. (11) is satisfied, where ΔE

$$V_{A-H}(n_{A-H}) = V_{B-H}(n_{B-H}) + \Delta E \quad (11)$$

is the energy difference between reactants and products. Obviously, $n_{A-H} = 1 - n_{B-H}$ and the relation between bond-orders and bond distances is obtained from eqn. (9) and (10). The $V_{A-H}(n_{A-H})$ and $V_{B-H}(n_{B-H})$ terms are diatomic-like functions characterizing the bonds being broken and formed, respectively. In this work, for simplicity, we will use Morse curves but more accurate forms can be employed. Morse curves are deemed sufficient for most reactions, although they may break down for very endo- or exoergic situations. The activation energy for each reaction is, thus, given by $V_{A-H}(n^{\ddagger}_{A-H})$, in the previous notation, or by the equivalent expression corresponding to products.

It may seem surprising that ISM does not explicitly contain triplet repulsion terms like some of the methods described above, or take into consideration zero point energy effects. The former are included through the use of a reduced distension, expressed through the proportionality between bond extensions and ($l_{A-H,eq} + l_{B-H,eq}$). In addition, the a' parameter was

calibrated so that experimental activation energies would be reproduced and, therefore, implicitly accounts for zero point energy differences.

Most of the models described in the previous section are used, and this work is no exception, to estimate activation energies. These are typically determined using data in the 400–1000 K range. For this range of temperatures, especially near the lower limit, quantum mechanical tunneling may be significant in the overall rates. Nuclear tunneling corrections can be incorporated in the model to account in detail for the increase in the thermal rate coefficient due to such effects.[54] However, in this work we focus on the comparison between calculated and experimental activation energies, assuming that the latter are dominated by thermal activation.

Input data

One of the strongest assets of ISM is its simplicity. This is reflected by the data required to calculate reaction energy barriers. They consist, for each reactive system, of the parameters that define the Morse curves for the two bonds considered, *i.e.*, the respective well depth, D_e, equilibrium inter-nuclear distance, l_{eq}, and the decaying parameter, β. For consistency, most of the bonds were defined using the critical selection of ref. 7. All the data pertaining to potential curves are summarized in Table 1.

Additionally, one must specify the value of the parameter m. This can be done, in some cases, using chemical arguments. The next two sections will be partly dedicated to the problem of estimating the total bond-order.

Results and discussion

Total bond-order $m = 1$

In this section we initially discuss the prototype reaction H + H$_2$ and also the attack of the hydrogen atom or hydrocarbon radicals on hydrocarbon molecules. In spite of the fact that these are well studied reactions, a full understanding of the structure–reactivity relationships is far from having been achieved. Systems in which heteroatoms are present in the reactant molecules, but not directly involved in the reactive bonds, are also considered in this first group.

These reactions are treated following the reaction between a hydrogen atom and a hydrogen molecule, that is, we *a priori* use $m = 1$. Thus, in what concerns the reactive bonds, we do not predict the H–H–H transition state to be essentially different from those of the H–H–C– or –C–H–C– types.

The ISM results for hydrocarbon reactions are summarized in Table 2 and Fig. 2(a), together with available experimental

Table 2 Results for hydrogen transfers involving H atoms, hydrogen molecules and hydrocarbons. The values indicated in columns 2 to 8 correspond, respectively, to the difference in well depth between reactants and products, reduced bond distension, reactant bond-order and reactant and product bond lengths at the transition state, calculated (this work) and literature values for the activation energies. The latter were experimentally determined, except where italicized; when several values are available, only extremes are indicated. All distances are presented in Å and energies in kJ mol^{-1}. In cases of ambiguity, the exchanged atoms are underlined

System	ΔE	η	$n^{\ddagger}_{A-H}$	$l^{\ddagger}_{A-H}$	$l^{\ddagger}_{B-H}$	$V(n^{\ddagger}_{A-H})$	E_a	Refs.
H + H$_2$	0.0	0.216	0.50	0.90	0.90	32.6	31.8–33.5	1, 55
H + CH$_4$	−4.1	0.216	0.51	1.28	0.94	44.3	41.8–49.8	1, 55
H + C$_2$H$_6$	−22.7	0.218	0.55	1.27	0.97	35.6	38.1–40.6	1, 55
H + CH$_3$C$\underline{H}_2$CH$_3$	−31.5	0.219	0.57	1.27	0.98	32.3	34.7–35.1	1, 6
H + (CH$_3$)$_3$CH	−43.7	0.222	0.59	1.27	1.00	28.0	29.3	6
H + PhH	21.2	0.218	0.46	1.30	0.91	58.2	36.4	1
(Ph + H$_2$	−21.2	0.218	0.54	0.91	1.30	37.0	27.2	1)
H + PhCH$_3$	−75.3	0.233	0.66	1.23	1.05	18.8	25.1	6
CH$_3$ + CH$_4$	0.0	0.216	0.50	1.32	1.32	61.1	53.6–62.3	1, 6, 7, 9, 55
CH$_3$ + C$_2$H$_6$	−18.6	0.217	0.53	1.31	1.34	51.8	45.2–50.6	1, 6, 7, 9, 55
CH$_3$ + CH$_3$C$\underline{H}_2$CH$_3$	−27.4	0.218	0.54	1.31	1.36	48.0	48.5	1
CH$_3$ + (CH$_3$)$_3$CH	−39.6	0.219	0.56	1.32	1.37	43.0	33.9–34.3	1, 6, 7, 9
CH$_3$ + PhCH$_3$	−71.2	0.226	0.62	1.27	1.42	31.9	35.1	23
C$_2$H$_5$ + C$_2$H$_4$	40.9	0.219	0.43	1.35	1.29	83.4	81.2	1, 10
C$_2$H$_5$ + C$_2$H$_6$	0.0	0.216	0.50	1.33	1.33	59.9	55.6	9
C$_2$H$_5$ + CH$_3$C$\underline{H}_2$CH$_3$	−8.8	0.216	0.51	1.34	1.34	55.7	47.7	9
C$_2$H$_5$ + (CH$_3$)$_3$CH	−21.0	0.217	0.53	1.34	1.36	50.0	41.8	9
C$_2$H$_5$ + PhCH$_3$	−52.6	0.222	0.59	1.29	1.40	37.4	38.9	6
CH$_3$CHCH$_3$ + CH$_3$C$\underline{H}_2$CH$_3$	0.0	0.216	0.50	1.35	1.35	60.1	34.7^a–54.0^b	1
(CH$_3$)$_3$C + (CH$_3$)$_3$CH	0.0	0.216	0.50	1.36	1.36	59.8	43.9	9
(CH$_3$)$_3$C + PhCH$_3$	−31.6	0.219	0.56	1.31	1.41	45.3	43.2	6
Ph + CH$_4$	−25.2	0.217	0.54	1.29	1.34	50.1	39.7–46.4	1, 6
Ph + PhH	0.0	0.216	0.50	1.31	1.31	62.4	66.1	9
PhCH$_2$ + PhCH$_3$	0.0	0.216	0.50	1.35	1.35	59.6	71.1	23
H + CH$_3$C$\underline{H}$O	−70.0	0.230	0.64	1.26	1.04	19.7	13.8	7
CH$_3$ + CH$_3$C$\underline{H}$O	−66.0	0.224	0.61	1.30	1.41	32.8	25.9–34.3	7
H + CH$_3$COCH$_2$H	−39.3	0.221	0.59	1.26	1.00	29.9	26.8	7
CH$_3$ + CH$_3$COCH$_2$H	−35.3	0.219	0.56	1.30	1.37	45.4	40.6	7
CH$_3$COCH$_2$ + PhCH$_3$	−35.9	0.219	0.56	1.31	1.39	44.4	38.9	23

^{a} CH$_3$CH$_2$CH$_2$ + CH$_3$C$\underline{H}_2$CH$_3$. ^{b} CH$_3$CHCH$_3$ + C$\underline{H}_3$CH$_2$CH$_3$.

activation energies‡ and some values calculated from other methods in the absence of experimental data. Also included are hydrogen atom transfers involving acetaldehyde and acetone, for which the agreement between calculated and experimental values is quite good. The presence of oxygen atoms close to the reactive bonds seems to have no net effect on the assumed bond-order. We note that the general agreement with experiment is quite good, and also that the Hammond postulate is followed for every reactive system.

Discrepancies between calculated and experimental values can, however, be found for some of the reactions. The largest difference appears in the H + benzene exchange. However, the experimental value is not consistent with that corresponding to the reverse reaction (also shown for completeness in Table 2), once the direct process has $\Delta E = 21.2$ kJ mol^{-1}. This is a direct consequence of the use of two different temperature intervals in the determinations for the direct (883 K $\leqslant T \leqslant$ 963 K) and reverse (453 K $\leqslant T \leqslant$ 623 K) reactions. Also, reaction between H$_2$ and the phenyl radical probably occurs through a process of addition followed by elimination, and not exchange. The identity reaction between *tert*-butyl and *tert*-butane presents a difference of *ca.* 12 kJ mol^{-1} between the calculated and the closest semi-empirical value (note that in this case comparison is not made with experiment). For the remaining cases, those differences are typically below 4 kJ mol^{-1}, including examples involving alkenes and aromatic compounds.

Some of the calculated bond distances can be compared with semi-empirical or *ab initio* results. For example, the ISM values are $l^{\ddagger}_{C-H} = 1.32$ Å for CH$_3$ + CH$_4$, against the MNDO-PM3[9] value of 1.275 Å, and for larger systems this difference may not be as significant, or may vary with the bonds considered. For ethyl + ethane we have $l^{\ddagger}_{C-H} = 1.33$ Å, the MNDO-PM3 value is
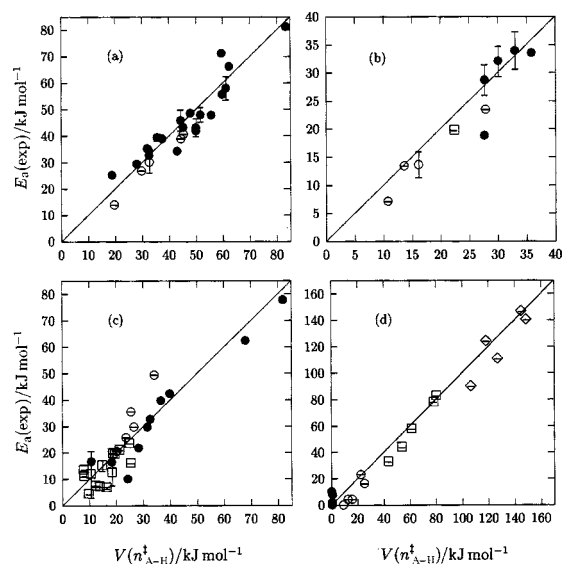

Fig. 2 Representation of the activation energy data of Tables 2, 3, 4 and 5: experimental *vs.* ISM (this work) determinations. Reactions in which data are not consistent or are estimated with similar reactions were not included. The solid line represents equality between abcissae and ordinate. Key: (a) (●), reactions involving hydrogen and/or hydrocarbons; (○), reactions involving hydrogen and/or aldehydes and ketones; (b) reactions in which the reactive bonds include Si (●), Sn (○) and Ge (□); (c) transition states of the N–H–H(C–) (○), –O–H–H(C–) (●) and –S–H–H(C–) (□) types; (d) reactions with halogen atoms [F (●), Cl (○), Br (□), I (◇)].

1.31, and for methyl + *tert*-butane the relation is 1.30, 1.40 Å to the semi-empirical values 1.253, 1.415 Å. In the case of ethyl + ethylene, *ab initio* estimates[10] point to 1.405, 1.293 while the corresponding ISM values are 1.35, 1.29 Å.

‡ The temperature range in which E_a was experimentally determined can be found in the original references.

Table 3 Same as Table 2, but for compounds in which carbon was replaced by atoms of the same group ($m = 1.12$). The values of the last column were taken from the compilation in ref. 7, except where indicated

System	ΔE	η	$n^{\ddagger}_{A-H}$	$l^{\ddagger}_{A-H}$	$l^{\ddagger}_{B-H}$	$V(n^{\ddagger}_{A-H})$	E_a
$CH_3 + H_3SiH$	-60.6	0.196	0.57	1.68	1.39	27.7	25.9–31.4
$C_2H_5 + H_3SiH$	-42.0	0.194	0.53	1.70	1.37	33.0	30.5–37.2
$CH_3 + (CH_3)_3SiH$	-48.9	0.194	0.54	1.71	1.36	30.1	29.3–34.7
$C_2H_5 + (CH_3)_3SiH$	-30.3	0.193	0.50	1.73	1.35	35.9	33.5
$CH_3CHCH_3 + (CH_3)_3SiH$	-21.5	0.193	0.49	1.74	1.35	39.3	*38.1*
$C_2H_5 + [(CH_3)_3Si]_3S$	-76.1	0.200	0.61	1.68	1.44	27.7	18.8
$H_3Si + H_3SiH$	0.0	0.193	0.50	1.77	1.77	48.8	*46.2*[a]–62.8
$CH_3 + (CH_3)_3SnH$	-123.9	0.207	0.65	1.87	1.50	13.6	13.4
$C_2H_5 + (CH_3)_3SnH$	-105.3	0.202	0.63	1.88	1.48	16.2	11.3–15.9
$Ph + (CH_3)_3SnH$	-149.1	0.214	0.69	1.85	1.53	10.8	7.1
$PhCH_2 + (CH_3)_3SnH$	-52.7	0.194	0.53	1.95	1.41	27.9	23.4
$C_2H_5 + (CH_3)_3GeH$	-74.9	0.198	0.59	1.73	1.42	22.4	19.7

[a] Ref. 16.

Compounds with silicon, tin or germanium

When carbon is replaced in the transition state by other atoms of the same group, the total bond-order m must be slightly increased. A 12% increase provides a bond-order similar to the one found in pseudo-alkenes[57,58] and is used here as a rough estimate for systems involving H-abstraction to or from Si, Sn and Ge ($m = 1.12$).

Table 3 presents the above results, which are also depicted in Fig. 2(b). The overall correspondence between calculated and experimental values is still observed, irrespective of the type of atom (Si, Sn or Ge) considered.

Hypervalency situations

For cases in which valence non-bonding electrons are available, the total bond-order at the transition state must be further increased.

Our estimate for m in these cases is based in very simple arguments. We consider $m = 1$ as corresponding to one chemical bond, resulting from the resonance forms:

$$X \downarrow\uparrow H \cdots Y \longleftrightarrow X \cdots H \uparrow\downarrow Y$$
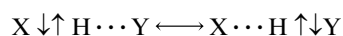
to which must be added the delocalization of one electron over the three atoms. We further assume that it is unlikely that more than four electrons can be located in the reactive bonds. For the latter situation we have thus $m = \frac{4}{3} = 1\frac{1}{3}$. This value is close to those previously found for proton exchange,[53] although employing different arguments. The presence of four electrons involved in the transition reactive bonds may readily be seen in the $O + H_2 \rightarrow OH + H$ reaction for which it is very likely that the transition species is similar to the water molecule.

It must be emphasized that increasing the total bond-order to describe some transition states is, essentially, a means of accounting for diverse stabilization factors. Amongst these, we refer the existence of non-linear geometries that allow the interaction between end-atoms or between non-bonding electrons in end-atoms and the reactive bonds[59] and also, to a lesser extent, dipole, multipole and strong van der Waals interactions.

A variety of systems for which this total bond-order has been applied can be found in Table 4. These results are also presented in Fig. 2(c). Once again, the majority of the calculated activation energies are close to the experimental determinations. However, some trends must be stressed: (i) for the –X–H–H type transition states the ISM estimates are sometimes too low, indicating probably an overestimated bond-order; (ii) when one of the reactive partners is NH_2, there is also a tendency to underestimate E_a; (iii) reactions in which PhSH is involved are characterized by high calculated activation energies. In the first case, reactions with a hydrogen atom as a reactant or product, substantial delocalization of electrons is prevented by the shortness of the chain containing the reactive bonds. For NH_2 attack, the non-bonding electrons in nitrogen do not extensively participate in the reactive bonds. In support of this, we note that the molecular orbital for the lone electron correlates with a $2p$ atomic orbital of nitrogen.[60] Although the value of m clearly exceeds 1 for these systems, the value $1\frac{1}{3}$ is excessive (except, perhaps, when the other partner is a molecule of considerable size). Finally, for the systems including thiophenol, delocalization of sulfur electrons seems to be increased by the proximity of the aromatic ring.

Other cases

We now turn to the analysis of other systems in which there is evidence that the simple picture discussed so far cannot be applied. Reactions of the type X + alkane $(H_2) \rightarrow HX$ + alkyl (H), in which X is a halogen atom, depend on the nature of the latter. When fluorine is the attacking atom, the reaction proceeds downhill, with low or negligible entrance barriers. For bromine and iodine, the situation is reversed and the reaction goes uphill, with an activation energy similar to the endoergicity. In terms of the ISM analysis, these three examples are probably extreme limits.

In what concerns the attack by chlorine atoms, the general trend is quite different. Activation barriers tend to be low, not exceeding 23 kJ mol^{-1} in the Cl + H_2 case, but the energy difference between reactants and products is also low. A high value $m = 2$ for the total bond-order has been previously found.[38,59] This value corresponds, tendentially, to the inflight H-atom being considered as bounded by two single bonds in the transition state, i.e., to an intensive delocalization of non-bonding electrons of the chlorine atom. The ISM prediction is, overall, too high except for the Cl + H_2 reaction. The results are summarized in Table 5 and Fig. 2(d), assuming $m = 2$.

A similar trend has been obtained by Zavitsas and Chatgilialoglu,[7] and a poor description of the HCl potential by Morse curves referred. However, we note that the well depth for HCl exceeds 400 kJ mol^{-1} and thus, the intersection is located not far from the equilibrium geometry of the product bond. In this zone it is unlikely that significant deviations of the Morse curves from the true potential are to be expected. In contrast, the fitting procedure of Roberts and Steel[6] predicts a negative activation energy for the attack of the chlorine atom on propane. Russell et al.[61,62] have also found negative activation energies in the corresponding reverse reactions with HBr and methyl, ethyl, isopropyl and isobutyl (for ethyl + HBr a more recent determination gives a small positive activation energy[2]). This has been attributed to the formation of an adduct in which both hydrogen and bromine are attached to the alkyl radical and still bonded to each other. A similar pattern of halogen

Table 4 Same as Table 2, but for compounds in which $m = 1\frac{1}{3}$ was considered

System	ΔE	η	$n^{\ddagger}_{A-H}$	$l^{\ddagger}_{A-H}$	$l^{\ddagger}_{B-H}$	$V(n^{\ddagger}_{A-H})$	E_a	Refs.
$NH_2 + H_2$	−8.9	0.162	0.51	0.88	1.16	25.5	35.5	6
$NH_2 + CH_4$	−13.0	0.162	0.51	1.25	1.19	34.2	49.4	6
$NH_2 + C_2H_6$	−31.5	0.164	0.56	1.24	1.21	26.6	29.9	6
$NH_2 + CH_3C\underline{H}_2CH_3$	−40.4	0.165	0.58	1.24	1.22	23.8	25.7	6
$NH_2 + (CH_3)_3CH$	−52.6	0.167	0.60	1.25	1.24	20.1	20.5	6
$H + H_2S$	−64.3	0.176	0.67	1.43	1.01	10.6	2.9–20.5	7
$H + CH_3SH$	−80.1	0.184	0.71	1.42	1.04	8.1	10.9	7
$H + (CH_3)_2CHSH$	−79.2	0.183	0.70	1.44	1.04	8.0	13.4	7
$CH_3 + H_2S$	−60.2	0.170	0.62	1.47	1.36	18.5	7.5–17.2	7
$CH_3 + CH_3SH$	−76.0	0.175	0.66	1.46	1.39	14.9	13.0–17.2	7
$C_2H_5 + CH_3SH$	−57.4	0.169	0.62	1.48	1.37	18.8	*19.7*	7
$CH_3CHCH_3 + CH_3SH$	−48.6	0.167	0.60	1.49	1.37	21.2	*20.9*	7
$(CH_3)_3C + CH_3SH$	−36.4	0.165	0.58	1.50	1.37	24.9	*23.4*	7
$C_2H_5 + CH_3CH_2SH$	−55.4	0.169	0.62	1.49	1.37	19.5	*19.2*	7
$CH_3 + PhSH$	−106.7	0.187	0.72	1.45	1.45	9.7	*4.2*	7
$C_2H_5 + PhSH$	−88.1	0.180	0.69	1.47	1.43	12.3	7.1–7.5	7
$CH_3CHCH_2 + PhSH$	−79.2	0.177	0.67	1.48	1.43	13.9	7.1	7
$(CH_3)_3C + PhSH$	−67.1	0.173	0.65	1.49	1.42	16.4	6.3–7.1	7
$PhCH_2 + PhSH$	−35.5	0.164	0.57	1.52	1.35	25.4	15.9	7
$O + H_2$	12.2	0.165	0.43	0.91	1.08	36.7	39.7	7
$OH + H_2$	−59.0	0.173	0.65	0.83	1.17	10.8	16.7	5
$OH + CH_4$	−63.1	0.169	0.62	1.20	1.19	18.4	16.5	56
$HOO + CH_4$	66.3	0.181	0.31	1.37	1.05	81.4	77.8	7
$CH_3O + CH_4$	−1.9	0.163	0.47	1.27	1.09	40.0	42.3	6
$CH_3O + C_2H_6$	−20.5	0.162	0.51	1.25	1.12	31.5	29.7	6
$CH_3O + CH_3C\underline{H}_2CH_3$	−29.4	0.163	0.53	1.26	1.13	28.3	21.8	1
$CH_3O + (CH_3)_3CH$	−41.5	0.164	0.56	1.26	1.14	24.3	10.0–23.8	6, 7
$CH_3COO + C_2H_6$	47.7	0.174	0.34	1.35	1.06	68.1	62.3	7

Table 5 Same as Table 2, for reactions involving the attack of a halogen atom ($m = 2$). Experimental data are from ref. 1

System	ΔE	η	$n^{\ddagger}_{A-H}$	$l^{\ddagger}_{A-H}$	$l^{\ddagger}_{B-H}$	$V(n^{\ddagger}_{A-H})$	E_a
$F + H_2$	−131.6	0.183	0.89	0.76	1.21	0.4	10.3
$F + CH_4$	−135.7	0.160	0.85	1.11	1.21	1.0	7.7
$F + C_2H_6$	−154.3	0.172	0.87	1.12	1.24	0.7	2.0
$F + CH_3CH_2CH_3$	−163.1	0.176	0.88	1.13	1.25	0.6	0.0
$F + (CH_3)_3CH$	−175.3	0.183	0.89	1.14	1.27	0.5	0.0
$Cl + H_2$	12.0	0.109	0.44	0.87	1.36	22.8	23.0
$Cl + CH_4$	7.9	0.108	0.47	1.23	1.39	25.3	16.3
$Cl + C_2H_6$	−10.7	0.109	0.56	1.20	1.42	16.0	4.2
$Cl + CH_3CH_2CH_3$	−19.5	0.111	0.59	1.20	1.44	12.8	4.1
$Cl + (CH_3)_3CH$	−31.7	0.115	0.64	1.20	1.47	9.3	0.1
$Br + H_2$	79.0	0.146	0.19	1.02	1.45	80.5	82.4
$Br + CH_4$	75.0	0.132	0.24	1.36	1.47	78.3	77.8
$Br + C_2H_6$	56.4	0.123	0.29	1.33	1.48	61.5	57.3
$Br + CH_3CH_2CH_3$	47.6	0.119	0.32	1.33	1.49	53.9	43.5
$Br + (CH_3)_3CH$	35.3	0.114	0.36	1.32	1.50	43.9	32.6
$I + H_2$	148.7	0.194	0.09	1.18	1.62	149.0	140.2
$I + CH_4$	144.6	0.170	0.13	1.52	1.63	145.4	146.4
$I + C_2H_6$	126.1	0.160	0.15	1.49	1.64	127.2	110.5
$I + CH_3CH_2CH_3$	117.2	0.155	0.16	1.49	1.64	118.5	123.8
$I + (CH_3)_3CH$	105.1	0.148	0.18	1.48	1.65	106.7	89.5

attack with low activation energies has been found in the $Cl + C_2H_4$ hydrogen exchange reaction.[63] In this case, one should also account for the rupture of the double bond in ethylene. The form in which ISM was applied in the present work cannot account for such mechanisms, and this discrepancy should be further analyzed in the future.

In the case of hydrogen abstractions of the RO–H + OR type, they are characterized both by a low energy of activation and a low pre-exponential Arrhenius factor as compared to situations in which carbon is involved. This has been attributed[7] to a low antibonding interaction between the O atoms and, thus, to the ability to form a tight transition state. Other explanations suggest the formation of a hydrogen-bonded complex formed prior to hydrogen transfer or electron transfer concerted with proton transfer.[9]

In any case, the approach used in ISM leads to energy barriers higher than the experimental values, as could have been anticipated. The same happens, although to a lesser extent, for the S–H–S type transition states. Our results are summarized in Table 6, where the value $m = 1.45$[59] has been used. This parameter could have been increased to accommodate the experimental values but we believe that the discrepancy is probably due to an alternative mechanism, as discussed above.

Extrapolation of the *m* parameter

As we have shown the *m* parameter is essentially the same for a specified type of transition state. For the types considered, $m = 1$ works as a lower limit and upper limits can easily be obtained through the use, for example, of Pross–Shaik type diagrams[64] in hypervalency situations. In the simple

Table 6 Same as Table 2, but for reactions with transition states of the –SHS– or –OHO– types ($m = 1.45$). Values for E_a taken from ref. 7

System	ΔE	η	$n_{\text{A–H}}^{\ddagger}$	$l_{\text{A–H}}^{\ddagger}$	$l_{\text{B–H}}^{\ddagger}$	$V(n_{\text{A–H}}^{\ddagger})$	E_a
HS + H$_2$S	0.0	0.149	0.50	1.53	1.53	36.5	31.0
CH$_3$S + CH$_3$SH	0.0	0.149	0.50	1.54	1.54	36.5	24.3
CH$_3$CH$_2$S + Ch$_3$CH$_2$SH	0.0	0.149	0.50	1.55	1.55	36.7	21.8
CH$_3$CH$_2$S + PhSH	−32.6	0.153	0.59	1.51	1.61	23.0	17.6
(CH$_3$)$_3$CO + (CH$_3$)$_3$COH	0.0	0.149	0.50	1.09	1.09	37.4	10.9

H(a) + H(b)–H(c)→H(a)–H(b) + H(c) reaction the orbitals involved are a nonbonding orbital, n, of the hydrogen atom and the σ and σ^* molecular orbitals in H$_2$, as illustrated.
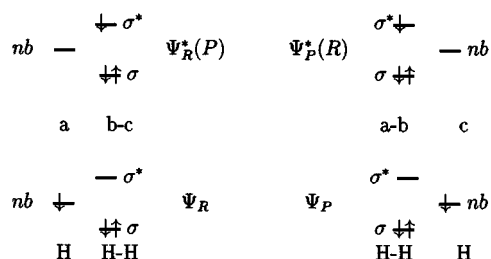

The lowest excited electronic configuration results from the promotion of the electron in the n orbital of the attacking H(a)-atom to the antibonding molecular orbital σ^*, in H(b)–H(c). Such a n–σ^* promotion helps the breaking of the H–H bond in the geometric configuration of the reactants. We denote it by $\Psi_R^*(P)$. Along the reaction path the σ-orbital of H(b)–H(c) develops a node between the two atoms and will correlate with the excited configuration $\Psi_P^*(R)$ of the products. The excited configurations dominate the transition-state electronic structure; each one has a chemical bond-order of $n^* = 1/2$, between the atoms b–c and a–b. Consequently $n^{\ddagger} = 1/2$.

The state correlation diagram for the reaction H(a) + H(b)–F(c)→H(a)–H(b) + F(c) can be constructed along similar lines, taking into account the number of nonbonding orbitals in the fluorine atom.
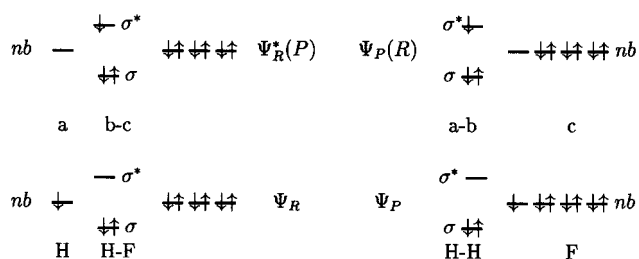
In the reactants configuration there are nonbonding orbitals in H(a) and F(c). Since some of these orbitals are not fully occupied, an interaction between them at the transition state leads to an electronic rearrangement; a new set of one bonding and one antibonding orbital is formed through the interaction of two nonbonding orbitals. Thus, the corresponding excited electronic configuration $\Psi_R^*(P)$ has a bond order $n^* = 1.5$ for b–c. From the products side there are only nonbonding orbitals in one of the atoms. Therefore, the conversion of nonbonding
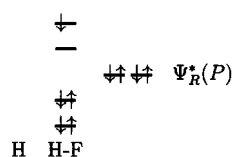
orbitals into bonding orbitals in the transition state through a strong resonance interaction is no longer possible. The excited state configuration $\Psi_P^*(R)$ possesses $n^* = 0.5$ between atoms a

and b. The transition state bond order is simply the average of these two values, $n^{\ddagger} = (1.5 + 0.5)/2 = 1$, or $m = 2$.

A similar view has been proposed by Dunning,[65] in which active and semi-active orbitals are considered. The latter are not directly involved in the bond transfer process but suffer energetically important changes on going from reactants to the linear saddle point.

For the H–H–O type transition states an intermediate situation between H$_3$ and H$_2$F is expected and, $e.g.$, for HF$_2$ we would have $m = 3$. These upper limits are in most cases excessive for practical use. It is more useful to extrapolate the value of m based solely on the transition-state type and a known activation energy of a prototype reaction of that type. In using such a scheme, one should make the difference between a RXHYR′ type transition state, in which R and R′ represent the chains linked to the X and Y atoms directly attached to the inflight hydrogen, and transition states for which R, R′ or both have been replaced for hydrogen. In this case m is midway between $m = 1$ and the corresponding value for longer chains. Such extrapolation would produce results that are closer to the experimental data than our previous guesses based on electronic considerations and we believe this procedure is helpful as a means to estimate reasonably accurate activation barriers with minimal input information.

Conclusions

We have applied the Intersection-State Model to a variety of hydrogen abstraction reactions with a view to monitoring the dependence of the energies of activation on the type of atoms present in the reactive bonds, and this variation on the structure of the transition state.

Reactions in which only hydrogen and carbon are present in the transition state, irrespective of the proximity of hetero-atoms, allowed the calculation of very accurate activation energies, employing the usual $m = 1$ BEBO total bond-order preservation. The replacement of carbon by atoms of the same group also led to very accurate estimates of the energy barrier, but in this case the total bond-order increases slightly at the transition state ($m = 1.12$). When an atom of nitrogen, oxygen or sulfur is present, the value of m must be further increased. We have found that assuming the presence of four electrons in the reactive bonds at the transition state ($m = 1.33$) provides good estimates for these systems, in which there is the participation of non-bonding electrons. However, if the heteroatom is present but the other reactive bond consists of –H–H, this increase is smaller ($m = 1.1$), indicating less delocalization of the available electrons.

For systems in which an inflight hydrogen atom is exchanged between two oxygen or sulfur atoms, the value of m must be increased towards values that are only compatible with the formation of stabilized adducts. A similar pattern was found for the attack of halogen atoms to hydrogen molecules or hydrocarbons. These cases confirm the existence of mechanisms other than the simple concerted bond-breaking/bond-forming process, as has been previously suggested in other studies.

In summary, we have shown how to use ISM both as a predictive tool, using $a priori$ estimates for the total bond-order at the transition state, and as an analytical tool, characterizing more complicated mechanisms.

Acknowledgements

References

1 C. H. Bamford and C. F. H. Tipper, ed., *Selected Elementary Reactions*, Elsevier, Amsterdam, 1975.
2 O. Dobis and S. W. Benson, *J. Phys. Chem.*, 1997, **A101**, 6030.
3 H. S. Johnston and C. Parr, *J. Am. Chem. Soc.*, 1963, **85**, 2544.
4 N. Agmon and R. D. Levine, *Isr. J. Chem.*, 1980, **19**, 330.
5 E. Kraka, J. Gauss and D. Cremer, *J. Chem. Phys.*, 1993, **99**, 5306.
6 B. P. Roberts and A. J. Steel, *J. Chem. Soc.*, *Perkin Trans. 2*, 1994, 2155.
7 A. A. Zavitsas and C. Chatgilialoglu, *J. Am. Chem. Soc.*, 1995, **117**, 10645.
8 M. L. McKee, A. Nicolaides and L. Radom, *J. Am. Chem. Soc.*, 1996, **118**, 10571.
9 D. M. Camaioni, S. T. Autray, T. B. Salinas and J. A. Franz, *J. Am. Chem. Soc.*, 1996, **118**, 2013.
10 J. P. A. Heuts, A. Pross and L. Radom, *J. Phys. Chem.*, 1996, **100**, 17087.
11 N. Luo, D. C. Kombo and R. Osman, *J. Phys. Chem.*, 1997, **A101**, 926.
12 O. Kondo and S. W. Benson, *Int. J. Chem. Kinet.*, 1984, **16**, 949.
13 J. Berkowitz, G. B. Ellison and D. Gutman, *J. Phys. Chem.*, 1994, **98**, 2744.
14 G. E. Davico, V. M. Bierbaum, C. H. DePuy, G. B. Ellison and R. R. Squires, *J. Am. Chem. Soc.*, 1995, **117**, 2590.
15 A. A. Zavitsas, *J. Chem. Soc.*, *Perkin Trans. 2*, 1996, 391.
16 B. P. Roberts, *J. Chem. Soc.*, *Perkin Trans. 2*, 1996, 2719.
17 A. A. Zavitsas, *J. Chem. Soc.*, *Perkin Trans. 2*, 1998, 499.
18 M. A. Evans and M. Polanyi, *Trans. Faraday Soc.*, 1938, **34**, 11.
19 R. P. Bell, *Proc. R. Soc. London*, 1936, **A154**, 414.
20 K. J. Laidler and J. C. Polanyi, *Prog. React. Kinet.*, 1965, **3**, 1.
21 H. S. Johnston, *Gas Phase Reaction Rate Theory*, Ronald, New York, 1966.
22 L. Pauling, *J. Am. Chem. Soc.*, 1947, **69**, 542.
23 R. D. Gilliom, *J. Am. Chem. Soc.*, 1977, **99**, 8399.
24 A. A. Zavitsas, *J. Am. Chem. Soc.*, 1972, **94**, 2779.
25 S. Schröder and W. Thiel, *J. Am. Chem. Soc.*, 1985, **107**, 4422.
26 K. A. Peterson and T. H. Dunning, *J. Phys. Chem.*, 1997, **A101**, 6280.
27 M. S. Gordon and D. G. Truhlar, *J. Am. Chem. Soc.*, 1986, **108**, 5412.
28 L. A. Curtiss, K. Raghavachari and J. A. Pople, *J. Chem. Phys.*, 1995, **103**, 4192.
29 A. L. J. Beckwith and A. A. Zavitsas, *J. Am. Chem. Soc.*, 1995, **117**, 607.
30 D. Dakternieks, D. J. Henry and C. H. Schiesser, *J. Chem. Soc.*, *Perkin Trans. 2*, 1997, 1665.
31 D. Dakternieks, D. J. Henry and C. H. Schiesser, *J. Chem. Soc.*, *Perkin Trans. 2*, 1998, 591.
32 D. Dakternieks, D. J. Henry and C. H. Schiesser, *Organometallics*, 1998, **17**, 1079.
33 Y. Chen, A. Rauk and E. Tschuikow-Roux, *J. Phys. Chem.*, 1991, **95**, 9900.
34 Y. Chen, E. Tschuikow-Roux and A. Rauk, *J. Phys. Chem.*, 1991, **95**, 9832.
35 A. J. C. Varandas and A. A. C. C. Pais, *Mol. Phys.*, 1988, **65**, 843.
36 A. J. C. Varandas and A. A. C. C. Pais, in *Theoretical and Computational Models for Organic Chemistry*, ed. S. J. Formosinho, I. G. Czismadia and L. G. Arnaut, Kluwer, Dordrecht, 1991, pp. 55–78.
37 A. A. C. C. Pais, A. I. Voronin and A. J. C. Varandas, *J. Phys. Chem.*, 1996, **100**, 7480.
38 A. J. C. Varandas and S. J. Formosinho, *J. Chem. Soc.*, *Faraday Trans. 2*, 1986, **82**, 953.
39 S. J. Formosinho and V. M. S. Gil, *J. Chem. Soc.*, *Perkin Trans. 2*, 1987, 1655.
40 S. J. Formosinho, *J. Chem. Soc.*, *Perkin Trans. 2*, 1987, 61.
41 S. J. Formosinho, *Tetrahedron*, 1987, **43**, 1109.
42 L. G. Arnaut and S. J. Formosinho, *J. Phys. Chem.*, 1988, **92**, 685.
43 S. J. Formosinho, *J. Chem. Soc.*, *Perkin Trans. 2*, 1988, 839.
44 K. Yates, *J. Phys. Org. Chem.*, 1989, **2**, 300.
45 S. J. Formosinho and L. G. Arnaut, *J. Chem. Soc.*, *Perkin Trans. 2*, 1989, 1947.
46 S. J. Formosinho, *J. Phys. Org. Chem.*, 1990, **3**, 325.
47 S. J. Formosinho, in *Theoretical and Computational Models for Organic Chemistry*, ed. S. J. Formosinho, I. G. Czismadia and L. G. Arnaut, Kluwer, Dordrecht, 1991, pp. 159–205.
48 L. G. Arnaut and S. J. Formosinho, *J. Phys. Org. Chem.*, 1990, **3**, 95.
49 L. G. Arnaut, *J. Phys. Org. Chem.*, 1991, **4**, 726.
50 L. G. Arnaut, in *Proton Transfer in Hydrogen-Bonded Systems*, ed. T. Bountis, Plenum, New York, NATO ASI, 1992, pp. 281–295.
51 L. G. Arnaut and S. J. Formosinho, *J. Photochem. Photobiol.*, 1992, **A69**, 41.
52 L. G. Arnaut and S. J. Formosinho, *J. Photochem. Photobiol.*, 1993, **A75**, 1.
53 L. G. Arnaut and S. J. Formosinho, in *Homogeneous Photocatalysis*, ed. M. Chanon, Wiley, New York, 1997, pp. 55–95.
54 S. J. Formosinho and L. G. Arnaut, *Adv. Photochem.*, 1991, **16**, 67.
55 G. L. Pratt, *Gas Kinetics*, Wiley, London, 1969.
56 V. S. Melissas and D. G. Truhlar, *J. Chem. Phys.*, 1993, **99**, 1013.
57 L. Pauling, *Proc. Natl. Acad. Sci. USA*, 1983, **80**, 3871.
58 G. Lendvay, *Chem. Phys. Lett.*, 1991, **181**, 88.
59 R. F. Nalewajski, S. J. Formosinho, A. J. C. Varandas and J. Mrozek, *Int. J. Quantum Chem.*, 1994, **52**, 1153.
60 G. Herzberg, *The Spectra and Structures of Simple Free Radicals*, Cornell, Ithaca, 1971.
61 J. J. Russell, J. A. Seetula, R. S. Timonen, D. Gutman and D. F. Nava, *J. Am. Chem. Soc.*, 1988, **100**, 3084.
62 J. J. Russell, J. A. Seetula and D. Gutman, *J. Am. Chem. Soc.*, 1988, **110**, 3092.
63 S. S. Parmar and S. W. Benson, *J. Phys. Chem.*, 1988, **92**, 2652.
64 A. Pross and S. S. Shaik, *Acc. Chem. Res.*, 1983, **16**, 363.
65 T. H. Dunning, *J. Phys. Chem.*, 1984, **88**, 2469.

Paper 8/07265E